Origin of the Photoacoustic Signal in Cytochrome P-450$_{cam}$: Role of the Arg186−Asp251−Lys178 Bifurcated Salt Bridge†

Carmelo Di Primo,*,‡ Eric Deprez,‡ Stephen G. Sligar,§ and Gaston Hui Bon Hoa‡

Institut de Biologie Physico-Chimique, INSERM-INRA U310, 13 rue Pierre et Marie Curie, 75005 Paris, France, and Departments of Biochemistry and Chemistry and Beckman Institute for Advanced Science and Technology, University of Illinois, Urbana, Illinois 61801

Received June 24, 1996; Revised Manuscript Received September 26, 1996⊗

ABSTRACT: The origin of the photoacoustic signal in ferrous CO−camphor−cytochrome P-450$_{cam}$ was investigated. Recently, the Arg186−Asp251−Lys178 bifurcated salt bridge, located above the heme pocket, has been shown to play a key role in the control of the diffusion step of camphor binding [Deprez, E., Gerber, N. C., Di Primo, C., Douzou, P., Sligar, S. G., & Hui Bon Hoa, G. (1994) *Biochemistry 33*, 14464−14468]. We considered the hypothesis that electrostriction resulting from the transient exposure of these charged residues to the solvent could be responsible for part of the photoacoustic signal. We thus examined the effects of a site-directed mutation of these linkages and ionic strength increases. Upon replacement of the Asp251 residue by an asparagine residue, the overall enthalpy and volume change of the CO dissociation reaction decrease from −5 to −24 kcal/mol and from 11 to 5.4 mL/mol, respectively. The mutation has the same effect on the thermodynamic parameters as increasing the ionic strength of the medium over a range of potassium or sodium concentrations from 0 to 500 mM. For the D251N mutant, the overall enthalpy of the reaction does not change with the ionic strength whereas a small effect is observed on the volume change. The results indicate that electrostriction around the bifurcated salt bridge contributes to the photoacoustic signal and suggest a scheme in which, following photodissociation of CO and diffusion of the molecule through the protein matrix, the structure relaxes and the bifurcated salt bridge desolvates.

Cytochrome P-450$_{cam}$ is a hemoprotein from *Pseudomonas putida* that catalyzes the formation of 5-*exo*-hydroxycamphor from camphor. The three-dimensional X-ray structure of this protein has been widely characterized in both the substrate-free (Poulos et al., 1986) and substrate-bound forms (Poulos et al., 1987) as well as when complexed with other ligands (Poulos & Howard, 1987; Raag & Poulos, 1989, 1991; Raag et al., 1993). Camphor strongly interacts with the protein via a hydrogen bond between its carbonyl group and the hydroxyl of Tyr96 and multiple hydrophobic contacts. This coupling links together the two regions of well-defined secondary structure reducing the flexibility of the protein.

Camphor access and binding to cytochrome P-450$_{cam}$ remain key questions for understanding catalysis. Despite the absence of a clear access channel as in cytochrome P-450$_{BM-3}$ (Ravichandran et al., 1993) [Poulos (1995) for review on cytochrome P-450s structures], the route to the non-solvent-exposed active site would be located in a depression made by the F/G loop, above the heme pocket. The opening and closing of this route would be controlled by a partially solvent-exposed bifurcated salt bridge between Asp251 (I helix), Arg186 (F/G loop), and Lys178 (F helix). This hypothesis is now supported by electrostatics calculations (Lounnas and Wade, unpublished results) and experiments that combined site-directed mutagenesis, ionic strength, and dielectric changes of the medium (Deprez et al., 1994).

If these ionic interactions are really involved in the conformational dynamics coupled to the binding and dissociation of substrates, one can expect the solvation of these charged groups to be altered. This would generate volume and heat changes resulting from the electrostriction of water molecules around them. Time-resolved photoacoustic calorimetry has been shown to be a useful tool for measuring volume and heat changes generated by conformational rearrangements that occur in the nanosecond to microsecond time scale (Peters et al., 1991; Braslavsky & Heibel, 1992). Recently, we used photoacoustic calorimetry to monitor the dynamics of cytochrome P-450$_{cam}$ triggered by the photoinduced dissociation of CO (Di Primo et al., 1993). We showed that, following the dissociation of this diatomic ligand, the protein undergoes large motions in the presence of camphor. However, the corresponding thermodynamic parameters could not be clearly assigned in terms of structural changes.

The goal of this work was to elucidate the origin of the photoacoustic signal in ferrous CO−camphor−cytochrome P-450$_{cam}$. Considering the hypothesis that electrostriction around transiently exposed charges might be responsible for part of the signal, cytochrome P-450$_{cam}$ was submitted to high ionic strength with sodium and potassium chloride to weaken the ionic interactions. The results were compared with those obtained with the site-directed mutant in which

† This work was supported by the Institut National de la Santé et de la Recherche Médicale, the Institut National de la Recherche Agronomique, European Community Biotechnology (Grant BIO2-CT94-2060, and the Actions Intégrées de Coopération Scientifique et Technique Procope (94116).

* Author to whom correspondence should be addressed. Telephone: +33-1-43 25 26 09. Fax: +33-1-43 29 80 88.

‡ INSERM-INRA U310.

§ University of Illinois.

⊗ Abstract published in *Advance ACS Abstracts,* December 15, 1996.

S0006-2960(96)01508-5 CCC: $14.00

the Arg186−Asp251−Lys178 bifurcated salt-bridge was removed by replacing the aspartate with an asparagine residue.

EXPERIMENTAL PROCEDURES

Cytochrome P-450$_{cam}$ wild type and D251N[1] mutant proteins were purified and generated as previously described (Gunsalus & Wagner, 1978). The pure concentrated proteins were stored at −80 °C with 20 mM β-mercaptoethanol, 240 mM potassium chloride, and 500 μM camphor in 50 mM potassium phosphate at pH 7.2. Substrate-free protein was obtained by passage of a pure concentrated sample through a Sephadex G-25 column equilibrated with the buffer used for the experiments, 100 mM Tris-HCl, at pH 7. Camphor was then added at a final concentration of 500 μM to ensure proper saturation of the protein. The ferrous CO−camphor−cytochrome P-450$_{cam}$ ternary complex was prepared by passing a stream of CO above the protein solution and then reduced with a solution of sodium dithionite. The concentration of protein currently used was 30 μM with a corresponding absorbance of 0.3 at 534 nm.

A new photoacoustic instrument was built and was inspired by the previous one (Di Primo et al., 1993). It uses a nitrogen-pumped dye laser (Laser Science) operating at 534 nm. As already shown (Di Primo et al., 1993), at this wavelength, the same sample can be used first in the ferric form as a calibration and then in the CO-bound form. An output energy of 5 μJ was chosen at a 2 Hz repetition rate. Two Peltier junctions were used to control the temperature within ±0.1 °C. The acoustic waves were detected by a 1 MHz piezoelectric ceramic transducer (Philips). The signals were amplified by a Panametric amplifier and recorded on a Lecroy 9400 oscilloscope. The data were analyzed on a personal computer with a new program.

In proteins, the photoacoustic signal, S, is given by

$$S = K(\Delta V_{th} + \Delta V_{conf}) \quad (1)$$

where K is the constant of the instrument response and ΔV_{th} is the thermal volume change produced by the heat, ΔE, deposited in the medium during the photoinduced reaction. ΔV_{conf} is related to conformational processes such as changes in the volume of the protein and/or electrostriction of exposed charges to the solvent. The photoacoustic response can be written as

$$S = K[(\beta/C_p\rho)\Delta E + \Delta V_{conf}] \quad (2)$$

where β is the thermal expansion coefficient of the solution, C_p the heat capacity, and ρ the density of the solution.

At a given temperature, $\varnothing$ is defined as the ratio of the signal arising from the sample of interest, S, over the signal of the calibration compound, S_{cal}, at the same temperature. The photoacoustic signal for the calibration compound is given by

$$S_{cal} = K(\beta/C_p\rho)E_{h\nu} \quad (3)$$

The quantum yield of CO escape out of the protein being 100% for all the different conditions of this work as it was measured (unpublished results), then

$$\varnothing = S/S_{cal} = (\Delta E/E_{h\nu}) + \Delta V_{conf}/[(\beta/C_p\rho)E_{h\nu}] \quad (4)$$

where $E_{h\nu}$ is the energy of the photon.

$\varnothing$ is temperature-dependent since β, C_p, and ρ are. If $F(T) = (\beta/C_p\rho)$, eq 4 becomes

$$E_{h\nu}\varnothing = \Delta E + \Delta V_{conf}/F(T) \quad (5)$$

A study of the photoacoustic signal as a function of the temperature will separate ΔE and ΔV_{conf}. The experiments were performed between 11 and 23 °C. For each condition of the medium, $\beta/C_p\rho$ was determined as described elsewhere (Westrick et al., 1990). The enthalpy change for the reaction, ΔH, is thus

$$\Delta H = E_{h\nu} - \Delta E \quad (6)$$

The experimental wave, $E(t)$, is the convolution of the instrument response, $T(t)$, obtained with the calibration compound with a time-dependent heat function, $H(t)$, which describes the heat decay of the photoinduced transients. $H(t)$ has the form

$$H(t) = \varnothing_1 + \sum_{i=2}^{n} \varnothing_n \exp(-t/\tau_n) \quad (7)$$

where $\varnothing_1$ corresponds to the heat deposition of all fast non-time-resolved processes (Rudzki, 1985).

The signals were successfully fitted with the two-step model

$$\text{E}-\text{CO} \xrightarrow{k_1} \text{E:CO} \xrightarrow{k_2} \text{E} + \text{CO}$$

where the relaxation time, $\tau_1 = 1/k_1$, is faster than the response time of the instrument (10 ns). Then eq 7 becomes

$$H(t) = \varnothing_1 + \varnothing_2 \exp(-t/\tau_2) \quad (8)$$

The procedure to find $\varnothing_1$, $\varnothing_2$, and τ_2 ($=1/k_2$) involves the convolution in the time domain of a calculated H(t), assuming only τ_2, with the instrument response, $T(t)$. The resulting calculated wave, $C(t)$, is then compared with the experimental wave and the fit evaluated by the sum of the square residuals. Compared with the fits with the prior program where three variables, $\varnothing_1$, $\varnothing_2$, and τ_2, had to be assumed to generate C(t), better fits were obtained with the new program, especially at the beginning of the signal (first quarter period). This probably explains why ΔV_1 and ΔH_1, in 100 mM Tris-HCl (pH 7) and 240 mM KCl, differ from the values already published (Di Primo et al., 1993).

Sperm whale myoglobin was used to validate this new apparatus and the fitting procedure. As reported in Table 1, our results agree well with those already published in the same buffer conditions (Westrick et al., 1990), despite the fact that the experiment was performed at a different wavelength, at a different concentration of protein, with a different laser beam geometry, with a different calibration compound, and in a different range of temperatures. This clearly indicates that, if the same chemical process is

[1] Abbreviations: WT, Cytochrome P-450$_{cam}$ wild type protein; D251N, mutant of cytochrome P-450$_{cam}$ in which aspartate 251 was replaced by an asparagine residue.

Table 1: Volume and Enthalpy Changes and Activation Parameters of the Cytochrome P-450$_{cam}$ Wild Type and D251N Mutant

	ΔV_1[a]	ΔH_1[b]	ΔV_2[a]	ΔH_2[b]	$\Delta H^{\ddagger}_2$[c]	$\Delta S^{\ddagger}_2$[d]
			P-450 WT			
none[e]	2.07 ± 0.22	4.5 ± 1.9	8.95 ± 0.53	−9.5 ± 4.5	7.9 ± 0.6	−0.14 ± 1.93
100 mM K_2HPO_4	1.02 ± 0.32	−3.9 ± 3.1	5.06 ± 0.48	−20.6 ± 4.6	6.9 ± 0.5	−3.44 ± 1.71
240 mM K^+	1.27 ± 0.19	−4.07 ± 1.52	5.56 ± 0.32	−28.5 ± 2.7	9.32 ± 0.27	5.0 ± 0.9
240 mM Na^+	1.30 ± 0.18	0.02 ± 1.72	4.5 ± 0.21	−25.8 ± 1.6	9.2 ± 0.7	4.6 ± 2.3
500 mM K^+	0.61 ± 0.13	2.96 ± 1.53	2.19 ± 0.22	−31.6 ± 2.7	8.32 ± 0.67	1.59 ± 2.31
500 mM Na^+	0.34 ± 0.08	−2.78 ± 1.01	1.76 ± 0.15	−25.8 ± 1.9	6.94 ± 0.54	−3.25 ± 1.83
			P-450 D251N			
none[e]	0.82 ± 0.20	1.54 ± 1.81	4.55 ± 0.35	−25.3 ± 3.1	7.9 ± 0.7	0.17 ± 2.28
500 mM K^+	0.28 ± 0.12	0.28 ± 1.50	1.61 ± 0.17	−23.6 ± 2.1	8.13 ± 0.55	0.78 ± 1.91
500 mM Na^+	0.22 ± 0.07	−0.97 ± 0.97	1.52 ± 0.15	−24.2 ± 2.1	8.59 ± 0.61	2.32 ± 2.13
myoglogin[f]	−9.2 ± 0.5	0.6 ± 2.2	15.0	10.7	11.1 ± 0.3	7.6 ± 1.9
myoglobin[g]	−6.2 ± 0.3	5.6 ± 0.9	13.8 ± 1.1	12.1 ± 3.3	11.3 ± 0.6	7.6 ± 1.9

[a] Milliliters per mole. [b] Kilocalories per mole. [c] Kilocalories per mole. [d] Calories per mole per kelvin. [e] In 100 mM Tris-HCl at pH 7. [f] Westrick et al. (1990). [g] This work.

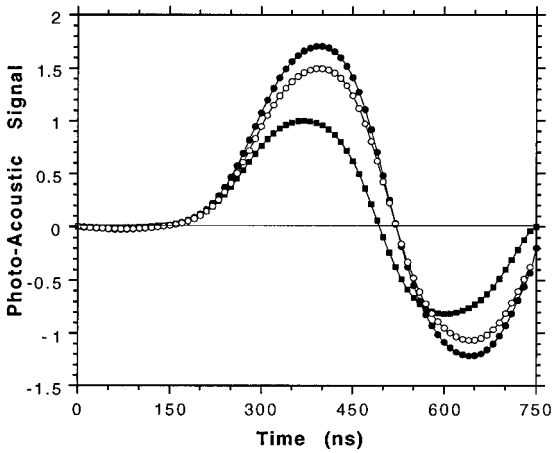

FIGURE 1: Photoacoustic spectra of camphor-bound cytochrome P-450$_{cam}$ at 17 °C in 100 mM Tris-HCl at pH 7. The signals were normalized by the maximum amplitude of the signal obtained with the calibration compound: (■) oxidized cytochrome P-450$_{cam}$ used as calibration compound, (○) ferrous CO−camphor−D251N mutant, and (●) ferrous CO−camphor−cytochrome P-450$_{cam}$.

monitored, the deduced thermodynamic parameters should not depend on the characteristics of the apparatus.

RESULTS

Typical photoacoustic spectra of cytochrome P-450$_{cam}$ in 100 mM Tris-HCl are presented in Figure 1. The signal obtained with the camphor-bound ferric form of the protein gives the instrument response. It corresponds to the fastest response obtained when the energy absorbed by the sample is only restored as heat without any conformational events. With the ferrous CO−camphor−cytochrome P-450$_{cam}$ ternary complex, chemistry is occurring in the time scale of the instrument response as indicated the time shift. The amplitude of the signal is higher. Replacement of Asp251 with an asparagine residue does not alter this shift, but the amplitude of the signal decreases significantly.

A two-step reaction was used as a minimal model to fit the photoacoustic signals according to the procedure described in Experimental Procedures. $\varnothing_1$ and $\varnothing_2$ are then plotted as a function of the temperature according to eq 5. The parameters deduced from these plots are the volume change, ΔV, and the enthalpy change, ΔH, for each step of the CO dissociation reaction. For clarity, only the variations of $E_{h\nu}\varnothing_1$ and $E_{h\nu}\varnothing_2$ as a function of $1/F(T)$ for the wild type protein and the D251N mutant without cation and in the presence of 500 mM sodium are presented in Figure 2. For all other conditions, the thermodynamic parameters deduced from similar plots are directly reported in Table 1. In this section, only the overall volume change, ΔV_{1+2} ($=\Delta V_1 + \Delta V_2$), and the overall enthalpy change, ΔH_{1+2} ($=\Delta H_1 + \Delta H_2$), will be analyzed. The thermodynamic parameters for each elementary step will be further analyzed in the Discussion.

For the wild type protein, ΔV_{1+2} decreases from 11 mL/mol without cation to 2.1 mL/mol in the presence of 500 mM sodium. ΔH_{1+2} decreases from −5.0 kcal/mol without cation to −28.6 kcal/mol in the presence of 500 mM sodium. Compared with that for the wild type protein, ΔV_{1+2} obtained with the D251N mutant without cation is smaller, 5.4 mL/mol. A small effect of sodium is observed on the volume change. ΔV_{1+2} decreases from 5.4 to 1.7 mL/mol in the presence of 500 mM sodium. ΔH_{1+2} does not change with sodium. Its value, −24 kcal/mol on average, is close to the one obtained with the wild type protein at high ionic strength. As reported in Table 1, within the experimental errors, similar results are obtained with potassium.

In order to establish whether the protonation or deprotonation of the buffer upon release or uptake of protons from the protein is contribuing to the signal, one experiment was carried out in 100 mM K_2HPO_4 buffer. If this occurs, the results should depend on the nature of the buffer since the volume change of protonation is negligible with Tris compared with the phosphate buffer (Neuman et al., 1973) and the heat of protonation is negligible with the latter compared with the former (Ort & Parson, 1979). Taking into account the observed ionic strength effect, only results obtained in similar or close ionic strength conditions are comparable. As reported in Table 1, the comparison of the results obtained in 100 mM phosphate buffer with those obtained in 100 mM Tris in the presence of 240 mM potassium or sodium, conditions where the corresponding ionic strengths are close, clearly indicates that no protonation or deprotonation of the buffer occurs during the reaction.

In Figure 3, we present a plot of the kinetic constant k_2 ($=1/\tau_2$) as a function of $1/RT$ for the wild type protein in the presence of 240 mM potassium which is roughly the standard condition of potassium concentration used in cytochrome P-450$_{cam}$ studies. The kinetic constant for the first step, k_1, is not available since the formation of the intermediate is assumed to occur faster than the response

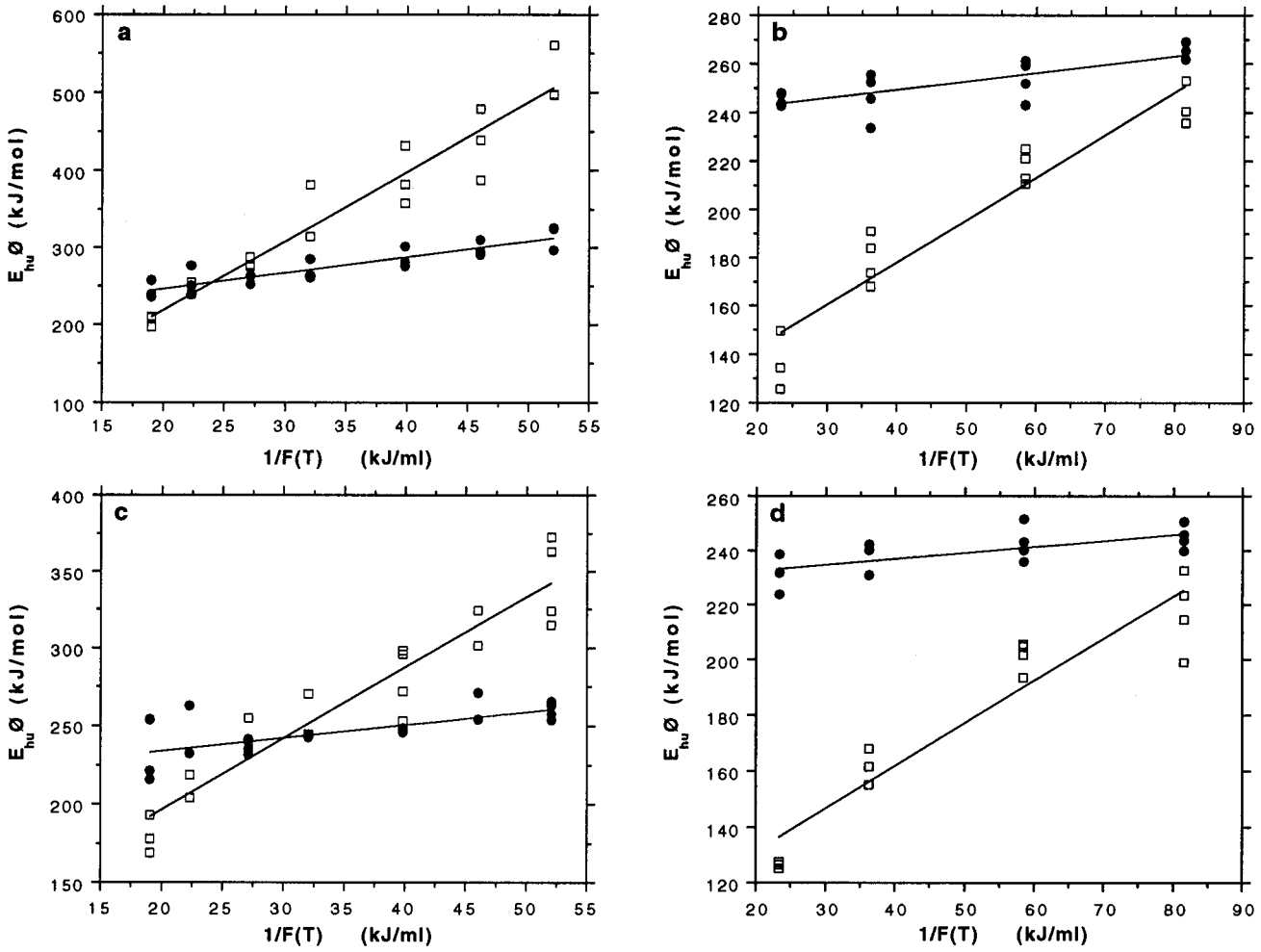

FIGURE 2: Plots of the $E_{h\nu}\varnothing$ versus 1/[$F(T)$]: (●) $E_{h\nu}\varnothing_1$ and (□) $E_{h\nu}\varnothing_2$. All the experiments were performed in 100 mM Tris-HCl at pH 7: (a) ferrous CO−camphor−cytochrome P-450$_{cam}$ wild type protein, (b) ferrous CO-camphor-cytochrome P-450$_{cam}$ wild type protein in the presence of 500 mM NaCl, and (c) ferrous CO−camphor−cytochrome P-450$_{cam}$ D251N mutant, and (d) ferrous CO−camphor−cytochrome P-450$_{cam}$ D251N mutant in the presence of 500 mM NaCl.

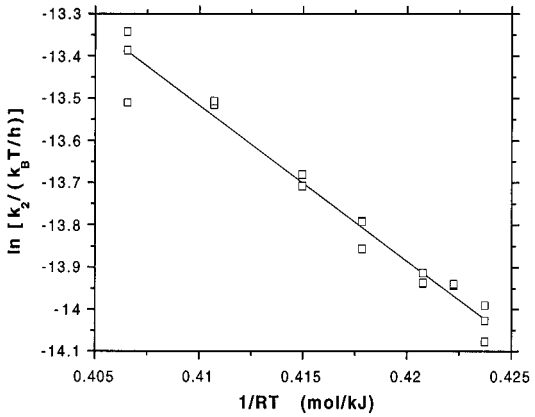

FIGURE 3: Plot of ln[k_2/[k_B(T/h)]] versus 1/RT for ferrous CO−camphor−cytochrome P-450$_{cam}$ in 100 mM Tris-HCl at pH 7 and 240 mM KCl. The experiments were performed between 11 and 23 °C.

time of the instrument. Between 23 and 11 °C, τ_2 changes from 110 to 210 ns, respectively. The activation parameters deduced from this variation are as follows: $\Delta H_2^{\ddagger} = 9.32 \pm 0.27$ kcal/mol and $\Delta S_2^{\ddagger} = 5.0 \pm 0.9$ cal mol^{-1} K^{-1}. The parameters obtained in all other conditions are reported in Table 1. $\Delta H_2^{\ddagger}$ does not significantly change with increasing concentrations of cations or with the mutation. The differences found for $\Delta S_2^{\ddagger}$ are attributable to experimental errors.

DISCUSSION

Cytochrome P-450$_{cam}$ is a well-characterized protein that has been used as a model to investigate responsivity to physicochemical perturbations (Marden & Hui Bon Hoa, 1982; Jung et al., 1996), the stereospecificity of the catalysis (Harris & Loew, 1995; Loida et al., 1995), the solvent accessibility of the heme pocket (Di Primo et al., 1992; Helms & Wade, 1995), and the mechanisms that control binding of large substrates to a totally buried active site in a protein that does not present any apparent pathway (Raag et al., 1993; Deprez et al., 1994). Diatomic ligands have been widely used as probes to investigate protein dynamics in hemoproteins such as myoglobin, hemoglobin (Mims et al., 1983; Kottalam & Case, 1988; Genberg et al., 1991; Traylor et al., 1992), and cytochromes P-450$_{cam}$ (Unno et al., 1994; Tian et al., 1995; Kato et al., 1995). In the latter, both CO and O_2 can bind in the active site together with large substrates of more than 10 carbons. The analysis of the CO−camphor−protein complex can then provide useful insight for understanding the physiological O_2−camphor−cytochrome P-450$_{cam}$ complex that cannot be investigated under standard conditions of medium and temperature.

The effects of camphor on the CO-binding reaction have been recently characterized by flash photolysis experiments (Unno et al., 1994; Tian et al., 1995; Kato et al., 1995) and FTIR spectroscopy (Jung et al., 1992). In summary, camphor

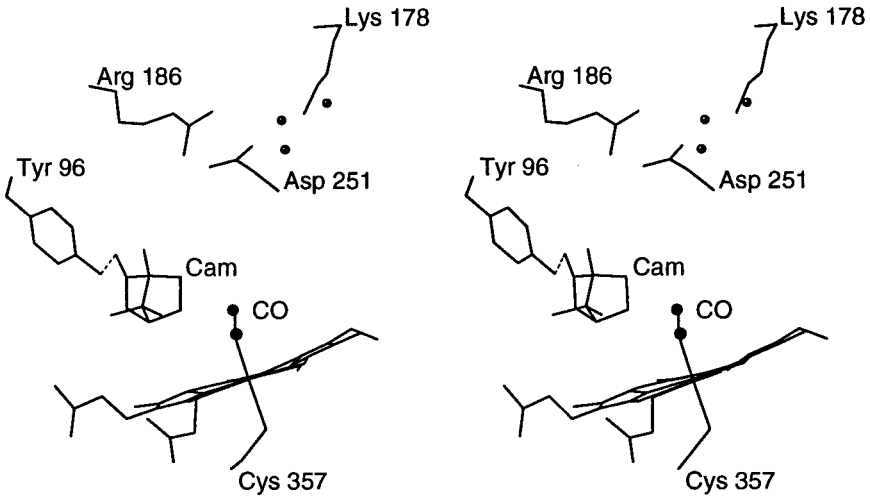

FIGURE 4: Stereoview of the active site of the CO−camphor−cytochrome P-450$_{cam}$ ternary complex which also shows the closest water molecules to the side chains of the Arg186−Asp251−Lys178 bifurcated salt bridge as solved by X-ray crystallography (Raag & Poulos, 1989). The three water molecules and the hydrogen bond between Tyr96 and camphor are represented by small balls and a dotted line, respectively. This figure was made with the Mage program (Richardson & Richardson, 1994) from the PDB file (Bernstein et al., 1977).

drastically decreases both the on and off rates of the bimolecular reaction, roughly 100- and 50-fold, respectively. The FTIR spectra of the CO stretching modes become sharper, indicating a reduced freedom of the CO molecule in the heme pocket. Of crucial importance is the result that camphor binding changes the amount of CO molecules that leave the protein upon photolysis from roughly 5 to more than 95% (Shimada et al., 1979; Tian et al., 1995).

In the prior investigation that used photoacoustic calorimetry, a time shift of the signal of ferrous CO-bound cytochrome P-450$_{cam}$, compared with that of the calibration compound, is detected only in the presence of camphor (Di Primo et al., 1993). Upon photolysis, an intermediate is formed which relaxes with a relaxation time near 120 ns at 20 °C. The nature of this intermediate as well as the exact origin of the photoacoustic signal were not clearly established. The aim of this work was to assign the photoacoustic signal to structural features of cytochrome P-450$_{cam}$ dynamics. Three elements were considered. First, photoacoustic calorimetry is sensitive to volume and enthalpy changes. Second, electrostriction around exposed charges generates volume and heat changes. Third, camphor access to the active site would be controlled by the partially solvent accessible Arg186−Asp251−Lys178 bifurcated salt bridge as shown in Figure 4. In other words, the dynamics of camphor-bound cytochrome P-450$_{cam}$, here triggered by the photolysis of the CO heme−iron bond, should generate volume and heat changes if during the reaction the solvation of the bifurcated salt bridge is altered.

Two sets of experiments were performed: the first one with the wild type protein increasing the ionic strength of the medium, with potassium and sodium, the second one, in similar conditions of medium, with the site-directed mutant in which the Arg186−Asp251−Lys178 bifurcated salt bridge was removed by replacing Asp251 with an asparagine residue.

Ionic Strength Effects on the Wild Type Protein. The effects of increasing ionic strengths on the thermodynamic parameters measured with photoacoustic calorimetry are clear. For the wild type protein, ΔV_{1+2} changes from 11 mL/mol without cations to 2.5 mL/mol, on average, at high ionic strengths. This effect suggests that electrostriction occurs during the conformational changes induced by the photodissociation of CO. A positive contribution to the overall volume change is suppressed when the ionic strength is increased. On the basis of results which show that when charges are exposed to the solvent the associated volume change is negative (Low & Somero, 1975; Heremans & Heremans, 1989; Rodgers & Sligar, 1991), the positive contribution to the overall volume change indicates that charges are desolvated during the reaction.

The effect of the ionic strength on the overall enthalpy change is important. ΔH_{1+2} changes from −5 kcal/mol without cation to −28 kcal/mol, on average, at high ionic strengths. Clearly, an endothermic process is suppressed when the ionic strength is increased. The solvation of charges being an exothermic reaction (Kebarle, 1977; Locke & McIver, 1983), again the variation of the overall enthalpy change with increasing ionic strengths indicates that charges are desolvated.

The photodissociation of CO from ferrous substrate-bound cytochrome P-450$_{cam}$ was recently investigated by flash photolysis experiments (Kato et al., 1995). The enthalpy change of the CO dissociation reaction in 100 mM potassium phosphate buffer is equal to −4.1 kcal/mol. In the same buffer condition, −24.5 kcal/mol (ΔH_{1+2}) is obtained with photoacoustic calorimetry. The origin of this discrepancy is not clear. However, the enthalpy change is not deduced from the same parameters. Photoacoustic calorimetry really measures the heat deposited along the reaction pathway, whereas in flash photolysis experiments, the enthalpy change is deduced from the variation of the rate constants as a function of the temperature.

Ionic Strength Effect on the D251N Mutant Protein. The results obtained with the D251N mutant confirm that changes in the solvation of exposed charges contribute significantly to the photoacoustic signal. Of the 11 mL/mol, 5.7 mL/mol ($\Delta V_{1+2}^{WT} - \Delta V_{1+2}^{D251N}$) comes from the desolvation of the Arg186−Asp251−Lys178 bifurcated salt bridge. A small effect of the cations is observed on the volume changes which suggests that somehow other ionic interactions still contribute to this parameter. However, these additional interactions do not contribute to the enthalpy change, ΔH_{1+2}, which remains unchanged. A similar observation can be made if the results

obtained with the wild type protein, in Tris buffer with 240 and 500 mM sodium or potassium, are compared. The increased ionic strength has an effect on ΔV but not on ΔH. This suggests that, in the intermediate-ionic strength condition, 240 mM cations, the bifurcated salt bridge is in a mutated-like structural conformation.

Ionic Strength and Mutation Effects on the Activation Parameters. Within the experimental errors, there is no effect of either the cations or the mutation on the kinetic constants of the second step and hence on the activation parameters. Obviously, the formation of the activated state does not involve breaking or formation of the bifurcated salt bridge. What does this kinetic step reflect? In the absence of camphor, CO does not leave the protein. CO quickly recombines to the heme iron with a rate equal to 4.3×10^7 s^{-1} as recently measured (Tian et al., 1995). Within the experimental error of this measurement, this geminate recombination rate is consistent with our previous findings (Di Primo et al., 1993) that, in the absence of camphor, chemistry is occurring in less than 10 ns which is the lower limit of the time scale of the instrument response. In the presence of camphor, 100% of the CO molecules leave the protein; the photoacoustic signal is shifted in time. It can be time-resolved. The kinetic process measured from the intermediate state formed upon photolysis has a rate equal to 8.6×10^6 s^{-1} ($k_2 = 1/\tau_2$) at 20 °C. In myoglobin, molecular dynamics simulations as well as flash photolysis experiments revealed that CO diffuses out of the protein from the geminate intermediate with a rate near 10^6-10^7 s^{-1} (Henry et al., 1983; Kottalam & Case, 1988; Traylor et al., 1992). CO dissociation from sperm whale myoglobin probed by photoacoustic calorimetry agrees with these results even if the possibility that this technique is not detecting exactly the same intermediate is discussed (Westrick et al., 1990). In cytochrome P-450$_{cam}$, CO leaves the protein with a rate equal to 29×10^6 s^{-1} (20−50% error margins) as measured by flash photolysis (Tian et al., 1995). This value is deduced from a geminate amplitude that represents only 2.5% of the overall absorbance change that occurs upon photolysis. In most cases, this amplitude is within the noise of the signal and is not detected. Then the rate of escape cannot be determined. With photoacoustic calorimetry, this rate can be accurately measured. In this work we found a value near 9×10^6 s^{-1}. All these results strongly suggest that the second kinetic process monitored with photoacoustic calorimetry corresponds to the migration of CO through the protein matrix from an intermediate similar to the geminate pair. The interpretation of the activation parameters remains difficult, but the positive value of $\Delta H^{\ddagger}$ and $\Delta S^{\ddagger}$ should reflect interatomic rearrangements that allow the CO molecule to escape from the heme pocket to the bulk solvent.

Structural Implications of the Measured Parameters. The study of the Arg45−heme propionate salt bridge mutant of sperm whale myoglobin probed by photoacoustic calorimetry revealed that the photodissociation of CO occurs according to a two-step process (Westrick et al., 1990). First, an intermediate is rapidly formed within 1 ns, and then, in a much slower process, CO diffuses out of the protein. The analysis of the thermodynamic parameters suggests that the salt bridge breaks during the first step and re-forms, during the second one, after the activated state. Even if the mutation drastically modifies the elementary enthalpy and volume changes, the overall parameters remain constant. In cytochrome P-450$_{cam}$, the mechanism is different. ΔH_{1+2} and ΔV_{1+2} are not equal for the wild type protein and the D251N mutant. These differences are mainly due to changes in ΔH_2 and ΔV_2, respectively. During the second step of the reaction, a 19 kcal/mol endothermic process occurs and charges are desolvated with a corresponding volume change equal to 5.7 mL/mol.

Derived from the thermodynamic parameters reported herein, the following mechanism is proposed for the photoinduced CO dissociation reaction. In the initial state, the bifurcated salt bridge would be solvated. Upon photolysis of the CO-heme iron bond, an intermediate is rapidly formed, possibly the geminate pair. The solvation of the bifurcated salt bridge does not significantly change. In a much slower rate-limiting process, CO diffuses through the protein matrix. Then the bifurcated salt bridge desolvates. Whether it closes raises the question of whether the desolvation of a salt bridge necessarily reflects the fact that the distance between the charges decreases. In a simple model, this will happen, but in a complex system such as a protein, steric constraints could prevent the charges from approaching one another. However, in cytochrome P-450$_{cam}$, this does not seem reasonable for a bifurcated salt bridge which would control the substrate access channel in a region that has to be flexible to accommodate an entrance. An alternative mechanism for the CO dissociation reaction could involve the concomitant opening of the salt bridge and the formation of the intermediate. But then it is not clear why the resulting energetic contribution is not seen in ΔH_1, the value of which, within the experimental error, does not change either with increasing ionic strength or the mutation. Even if the reaction is too fast to be time-resolved, the photoacoustic calorimeter is still sensitive to the heat rapidly deposited or absorbed. Hence, it should be detected. Furthermore, it is not clear either why ΔV_1 does not reflect this opening. ΔV_1 should increase and not decrease with increasing ionic strengths and with the mutation.

Does camphor leave the protein with the concomitant photoinduced expulsion of CO, or does it stay in the heme pocket and relax from the constrained position it adopts in the ternary complex to a nonconstrained one? Our results cannot answer this question. Until now, only one study suggests that camphor could be expulsed with CO (Wells et al., 1992). When resonance Raman spectra of ferrous CO−camphor−cytochrome P-450$_{cam}$ are collected from a sample cell which remains static with respect to the light source of analysis, the spectra have contributions from both the ferrous-free protein and the ferrous CO-bound protein, while these contributions are not seen when the cell is spinning. Preliminary investigations of the CO−camphor−protein complex, by flash photolysis experiments, seem to indicate that camphor does not leave the protein upon photolysis (unpublished results).

Now it should be remembered that the two three-dimensional structures of interest for this work, ferrous camphor-free and -bound, are not known. The closest ones without CO, ferric camphor-free and -bound, were solved from the ferric camphor-bound crystal in which, for the free protein, the substrate was diffused out by dialysis. The CO−camphor−protein ternary complex was also solved from this crystal by diffusing in CO. Therefore, the only possible comparison is between ferric camphor-bound and camphor-free and the ternary complex. This does not show differences

in the salt bridges. Nevertheless, the X-ray three-dimensional structure of the ternary complex shows that camphor moves by 0.8 Å from the position it adopts in the ferric substrate-bound protein (Raag & Poulos, 1989). The temperature factors of its carbon atoms increase by 50%. The region around Thr185 which involves the bifurcated salt bridge is more flexible and slightly expanded. Could these structural rearrangements be enough to force the solvation of the Arg186−Aps251−Lys178 bifurcated salt bridge? In an attempt to understand the catalytic mechanism of oxygen activation, a model was proposed for the physiological O_2−camphor−cytochrome P-450$_{cam}$ ternary complex which attributes a key role for this bifurcated salt bridge to a proton relay. This model implicates partial disruption of these linkages and new interactions with water molecules (Gerber & Sligar, 1994). Does this also occur in the CO−camphor−protein ternary complex, a mimic for the physiological one?

In conclusion, we have shown that electrostriction around charges contributes to the amplitude of the photoacoustic signal in ferrous CO−camphor−cytochrome P-450$_{cam}$. A significant part of it may be attributed to the desolvation of the Arg186−Asp251−Lys178 bifurcated salt bridge. The phase shift of the signal compared with the calibration signal reflects a slow kinetic process that would correspond to the migration of CO through the protein matrix from the geminate pair intermediate. Further experiments are required to ascertain whether camphor leaves the protein concomitantly with the expulsion of CO or stays inside the heme pocket.

ACKNOWLEDGMENT

We gratefully thank P. Debey and J. and J. Kornblatt for a critical reading of the manuscript. C. Tétreau, D. Lavalette, and M. Marden are thanked for helpful discussions and the opportunity they gave us to run flash photolysis experiments. We thank C. Barret, P. Regnier, and his team for the help provided for the generation and the purification of the wild type protein. We thank O. Krueger and C. and C. Jung for the gift of the program used to analyze the data and T. Cao, who adapted it to our experiments. T. Poulos, R. Wade, and V. Lounnas are thanked for their comments on the cytochrome P-450$_{cam}$ structures.

REFERENCES

Berstein, F. C., et al. (1977) *J. Mol. Biol. 112*, 535−542.
Braslavsky, S. E., & Heibel, G. E. (1992) *Chem. Rev. 92*, 1381−1410.
Deprez, E., Gerber, N. C., Di Primo, C., Douzou, P., Sligar, S. G., & Hui Bon Hoa, G. (1994) *Biochemistry 33*, 14464−14468.
Di Primo, C., Hui Bon Hoa, G., Douzou, P., & Sligar, S. G. (1992) *Eur. J. Biochem. 209*, 583−588.
Di Primo, C., Hui Bon Hoa, G., Deprez, E., Douzou, P., & Sligar, S. G. (1993) *Biochemistry 32*, 3671−3676.
Genberg, L., Richard, L., McLendon, M. C., & Dwayne Miller, R. J. (1991) *Science 251*, 1051−1054.
Gerber, N. C., & Sligar, S G. (1994) *J. Biol. Chem. 269*, 4260−4266.
Gunsalus, I. C., & Wagner, G. C. (1978) *Methods Enzymol. 52*, 116−188.
Harris, D., & Loew, G. (1995) *J. Am. Chem. Soc. 117*, 2738−2746.
Helms, V., & Wade, R. (1995) *Biophys. J. 68*, 810−824.
Henry, E. R., Sommer, J. H., Hofrichter, J., & Eaton, W. (1983) *J. Mol. Biol. 166*, 443−451.
Heremans, L., & Heremans, K. (1989) *Biochim. Biophys. Acta 999*, 192−197.
Jung, C., Hui Bon Hoa, G., Schröder, K. L., Simon, M., & Doucet, J. B. (1992) *Biochemistry 31*, 12855−12862.
Jung, C., Ristau, O., Schulze, H., & Sligar, S. G. (1996) *Eur. J. Biochem. 235*, 660−669.
Kato, M., Makino, R., & Iizuka, T. (1995) *Biochim. Biophys. Acta 1246*, 178−184.
Kebarle, P. (1977) *Annu. Rev. Phys. Chem. 28*, 445−476.
Kottalam, J., & Case, D. A. (1988) *J. Am. Chem. Soc. 110*, 7690−7697.
Locke, M. J., & McIver, R. T., Jr. (1983) *J. Am. Chem. Soc. 105*, 4226−4232.
Loida, P. J., Sligar, S. G., Paulsen, M. D., Arnold, G. E., & Ornstein, R. L. (1995) *J. Biol. Chem. 270*, 5326−5330.
Low, P. S., & Somero, G. N. (1975) *Proc. Natl. Acad. Sci. U.S.A. 72*, 3014−3018.
Marden, M. C., & Hui Bon Hoa, G. (1982) *Eur. J. Biochem. 129*, 111−117.
Mims, M. P., Porras, A. G., Olson, J. S., Noble, R. W., & Peterson, J. A. (1983) *J. Biol. Chem. 258*, 14219−14232.
Neuman, R. C., Kauzman, W., & Zipp, A. (1973) *J. Phys. Chem. 77*, 2687−2691.
Ort, D. R., & Parson, W. W. (1979) *Biophys. J. 25*, 355−364.
Peters, K. S., Watson, T., & Marr, K. (1991) *Annu. Rev. Biophys. Biophys. Chem. 20*, 343−362.
Poulos, T. L. (1995) *Curr. Opin. Struct. Biol. 5*, 767−774.
Poulos, T. L., & Howard, A. J. (1987) *Biochemistry 26*, 8165−8174.
Poulos, T. L., Finzel, B. C., & Howard, A. J. (1986) *Biochemistry 25*, 5314−5322.
Poulos, T. L., Finzel, B. C., & Howard, A. J. (1987) *J. Mol. Biol. 195*, 687−701.
Raag, R., & Poulos, T. L. (1989) *Biochemistry 28*, 917−922.
Raag, R., & Poulos, T. L. (1991) *Biochemistry 30*, 2674−2684.
Raag, R., Li, H., Jones, B. C., & Poulos, T. L. (1993) *Biochemistry 32*, 4571−4578.
Ravichandran, K. G., Boddupalli, S. S., Hasemann, C. A., Peterson, J. A., & Deisenhofer, J. (1993) *Science 261*, 731−736.
Richardson, D. C., & Richardson, J. S. (1994) *Trends Biochem. Sci. 19*, 135−138.
Rodgers, K. K., & Sligar, S. G. (1983) *J. Biol. Chem. 258*, 3599−3601.
Rudzki, J. E. (1985) Ph.D. Thesis, Harvard University, Cambridge, MA.
Shimada, H., Iizuka, T., Ueno, R., & Ishimura, Y. (1979) *FEBS Lett. 98*, 290−294.
Tian, W. D., Wells, A. V., Champion, P. M., Di Primo, C., Gerber, N. C., & Sligar, S. G. (1995) *J. Biol. Chem. 270*, 8673−8679.
Traylor, T. G., Madge, D., Taube, D. J., Jongeward, K. A., Bandyopadhyay, D., Luo, J., & Walda, K. N. (1992) *J. Am. Chem. Soc. 114*, 417−429.
Unno, M., Ishimori, K., Ishimura, Y., & Morishima, I. (1994) *Biochemistry 33*, 9762−9768.
Wells, A. V., Li, P., Champion, P. M., Martinis, S. A., & Sligar, S. G. (1992) *Biochemistry 31*, 4384−4393.
Westrick, J. A., Peters, K. S., Ropp, J. D., & Sligar, S. G. (1990) *Biochemistry 29*, 6741−6746.

BI961508A